James Madison University

From the SelectedWorks of Ray Enke Ph.D.

2013

Conditional knockdown of DNA methyltransferase-1 (Dnmt1) reveals a key role of retinal pigment epithelium in mammalian photoreceptor differentiation

I. O Nasonkin
S. L Merbs
K. Lazo
V. F Oliver
M. Brooks, et al.

Available at: https://works.bepress.com/raymond_enke/4/

Development 140, 1330-1341 (2013) doi:10.1242/dev.086603
© 2013. Published by The Company of Biologists Ltd

Conditional knockdown of DNA methyltransferase 1 reveals a key role of retinal pigment epithelium integrity in photoreceptor outer segment morphogenesis

Igor O. Nasonkin[1], Shannath L. Merbs[2], Kevin Lazo[1], Verity F. Oliver[2], Matthew Brooks[1], Krushangi Patel[1], Raymond A. Enke[2], Jacob Nellissery[1], Milan Jamrich[3], Yun Z. Le[4], Kapil Bharti[5], Robert N. Fariss[6], Rivka A. Rachel[1], Donald J. Zack[7], Enrique J. Rodriguez-Boulan[8] and Anand Swaroop[1,*]

SUMMARY

Dysfunction or death of photoreceptors is the primary cause of vision loss in retinal and macular degenerative diseases. As photoreceptors have an intimate relationship with the retinal pigment epithelium (RPE) for exchange of macromolecules, removal of shed membrane discs and retinoid recycling, an improved understanding of the development of the photoreceptor-RPE complex will allow better design of gene- and cell-based therapies. To explore the epigenetic contribution to retinal development we generated conditional knockout alleles of DNA methyltransferase 1 (*Dnmt1*) in mice. Conditional *Dnmt1* knockdown in early eye development mediated by *Rx-Cre* did not produce lamination or cell fate defects, except in cones; however, the photoreceptors completely lacked outer segments despite near normal expression of phototransduction and cilia genes. We also identified disruption of RPE morphology and polarization as early as E15.5. Defects in outer segment biogenesis were evident with *Dnmt1* exon excision only in RPE, but not when excision was directed exclusively to photoreceptors. We detected a reduction in DNA methylation of LINE1 elements (a measure of global DNA methylation) in developing mutant RPE as compared with neural retina, and of *Tuba3a*, which exhibited dramatically increased expression in mutant retina. These results demonstrate a unique function of DNMT1-mediated DNA methylation in controlling RPE apicobasal polarity and neural retina differentiation. We also establish a model to study the epigenetic mechanisms and signaling pathways that guide the modulation of photoreceptor outer segment morphogenesis by RPE during retinal development and disease.

KEY WORDS: Retina development, DNA methylation, Cell-cell interaction, Morphogenesis, Epigenetics, Mouse

INTRODUCTION

In retinal and macular neurodegenerative diseases, such as retinitis pigmentosa (RP) and age-related macular degeneration (AMD), vision loss ultimately results from the dysfunction and/or death of photoreceptor cells (Jackson et al., 2002; Bramall et al., 2010; Wright et al., 2010). Rod and cone photoreceptors in the retina are highly polarized neurons that initiate the visual process (Lamb et al., 2007). To maximize photon capture, the photoreceptors contain unique structures, called outer segments (OSs), that utilize membrane discs to organize the visual pigment opsin and other phototransduction components for maximal efficiency (Palczewski et al., 1999; Luo et al., 2008). Each day, ~10% of OS discs are shed and then regenerated in a circadian manner in the mammalian retina (Young, 1974; Besharse et al., 1977; Bok, 1993). The retinal pigment epithelium (RPE) serves numerous essential roles in maintaining the health and function of photoreceptors, including acting as a barrier between photoreceptors and choroidal blood circulation, removing shed OSs and mediating retinoid recycling (Strauss, 2005; Sparrow et al., 2010).

The neural retina and RPE originate from anterior neuroectoderm, and their lineages separate at the late optic vesicle stage during eye development (Chow and Lang, 2001). Distinct pools of multipotent retinal progenitor cells (RPCs) acquire competence to produce specific sets of neurons in a defined order under the combined influence of intrinsic program(s) and extrinsic factors (Livesey and Cepko, 2001; Marquardt and Gruss, 2002; Wallace, 2011). Specific cell fates are determined by combinatorial actions of a select set of transcription factors. OTX2, RORβ, BLIMP1 (PRDM1) and CRX are among the regulatory proteins that are crucial for photoreceptor development (Swaroop et al., 2010); however, two key transcription factors – NRL and TRβ2 (encoded by *Thrb*) – together determine the generation of three distinct types of photoreceptors (rods, S-cones and M-cones) from postmitotic precursors (Ng et al., 2011). Downstream targets of NRL and CRX, as well as signaling proteins that modify their activity, further modulate the expression of photoreceptor genes (Oh et al., 2008; Onishi et al., 2009; Onishi et al., 2010; Roger et al., 2010; Hao et al., 2011). Loss or altered function of these regulatory proteins results in photoreceptor dysfunction and retinal diseases (Swaroop et al., 2010; Wright et al., 2010). Recent studies have begun to define the transcriptional regulatory networks that dictate photoreceptor development and homeostasis (Corbo et al., 2010; Hu et al., 2010; Hao et al., 2012; Hwang et al., 2012). Despite increasing interest in the role of epigenetic mechanisms (Cvekl and Mitton, 2010; Merbs et al., 2012; Nickells and Merbs, 2012; Popova et al., 2012), the role

[1]Neurobiology-Neurodegeneration and Repair Laboratory (N-NRL), National Eye Institute, National Institutes of Health, Bethesda, MD 20892, USA. [2]Division of Oculoplastic Surgery, Wilmer Eye Institute, Johns Hopkins University, Baltimore, MD 21287, USA. [3]Department of Molecular and Human Genetics, Baylor College of Medicine, Houston, TX 77030, USA. [4]Dept of Medicine, University of Oklahoma Health Sciences Center, Oklahoma City, OK 73104, USA. [5]Unit on Ocular Stem Cells and Translational Research, National Eye Institute, Bethesda, MD 20892, USA. [6]Biological Imaging Core, National Eye Institute, Bethesda, MD 20892, USA. [7]Departments of Ophthalmology, Molecular Biology and Genetics, Neuroscience, and Institute of Genetic Medicine, Johns Hopkins University, Baltimore, MD 21287, USA and Institut de la Vision, Université Pierre et Marie Curie, Paris, France. [8]Dyson Vision Research Institute, Weill Cornell Medical College, New York, NY 10065, USA.

*Author for correspondence (swaroopa@nei.nih.gov)

Accepted 15 January 2013

of the epigenome, if any, in establishing retinal cell fate, differentiation and/or homeostasis is yet to be elucidated.

We have been exploring the role of DNA methylation in RPE and photoreceptor development (Nasonkin et al., 2011; Merbs et al., 2012). Specification of pigmented RPE cells is an early event in eye morphogenesis (Bharti et al., 2006; Fuhrmann, 2010). Defects in the RPE monolayer, caused by partial genetic ablation of RPE in 6-week-old mouse eyes, can lead to photoreceptor degeneration (Longbottom et al., 2009). However, a direct developmental relationship between RPE and photoreceptors has not been established. Previous studies indicated that when RPE fails to specify (for example, in *Mitf* mutants) or when RPE development is abrogated by ectopic expression of diphtheria toxin, retinal development and photoreceptor maturation are severely compromised (Raymond and Jackson, 1995; Bumsted et al., 2001). Similarly, in retinal organotypic cultures, RPE is required for photoreceptor differentiation and survival (Ogilvie et al., 1999; Bandyopadhyay and Rohrer, 2010). Although the role of RPE in photoreceptor homeostasis is well established, genetic or epigenetic mechanisms that guide the development of the intricate photoreceptor-RPE complex are poorly understood.

DNA methylation and histone modifications are key epigenetic regulators that modulate the ability of transcription factors to gain access to DNA sites at which they act (Jaenisch and Bird, 2003; Bernstein et al., 2007). DNA methyltransferase (DNMT) 3a and 3b contribute to *de novo* methylation, whereas DNMT1 targets hemi-methylated CpGs during DNA replication, resulting in identical methylation patterns in the daughter DNA strands. Loss of function of *Dnmt1* in mice leads to embryonic lethality (Li et al., 1992), consistent with the established roles of DNMTs in organogenesis and disease (Robertson, 2005; Ma et al., 2010). DNMT1 is expressed at high levels in postmitotic neurons and is suggested to control their survival (Hutnick et al., 2009; D'Aiuto et al., 2011). However, the *in vivo* relevance of DNMT1 in neuronal cell fate determination and functional maturation is poorly understood.

While exploring the role of *Dnmt1* in retinal development, we developed a new mouse model that exhibits appropriate lamination and cell layers in the retina but shows compromised RPE differentiation and an absence of photoreceptor OSs. Using a comprehensive set of *Cre* lines to knockdown *Dnmt1* in RPE or neural retina, together with gene profiling and pyrosequencing of genomic DNA, we demonstrate a direct role of RPE in modulating photoreceptor OS biogenesis and identify candidate RPE genes that might play a role in this process. Our model should be useful in investigating the epigenetic control of photoreceptor-RPE architecture and in ascertaining the signaling molecules required for OS morphogenesis that are crucial for photoreceptor survival.

MATERIALS AND METHODS

Animals

All procedures with mice were performed in accordance with protocols approved by the National Eye Institute Animal Care and Use Committee. The mouse lines have been described previously: *Dnmt1*$^{fl/fl}$ (Jackson-Grusby et al., 2001), *Rx-Cre* (Swindell et al., 2006), *Pax6-[α] Cre* (Marquardt et al., 2001), *VMD2-Cre* (Le et al., 2008), *Six3-Cre* (Furuta et al., 2000) and *Crx-Cre* (Nishida et al., 2003).

Oligonucleotide primers

Primers used for amplifying genomic DNA, RT-PCR and pyrosequencing are listed in supplementary material Table S1.

Immunohistochemistry (IHC), histology and electron microscopy (EM)

Retinal histology was performed by fixing retinas for 30 minutes in paraformaldehyde (4% in PBS), followed by storage in 4% glutaraldehyde until processing. Tissues were embedded in methacrylate, sectioned at 1 μm, then counterstained with Hematoxylin and Eosin (H&E). EM was performed as described (Fariss et al., 1990). IHC procedures were as described (Nasonkin et al., 2011) and antibodies are listed in supplementary material Table S2.

Quantitative (q) RT-PCR and microarray data

RNA was prepared from neural retina (NR) or RPE/choroid from four *Dnmt1*$^{fl/fl}$ (control) and four *Dnmt1*$^{fl/fl}$*:Rx-Cre/+* (experimental) animals at each chosen time point using the RNeasy Mini Kit (Qiagen, Valencia, CA, USA). RNA quality and quantity were assessed using the BioAnalyzer 2100 RNA NanoChip (Agilent Technologies, Santa Clara, CA, USA) and Nanodrop (Thermo Scientific, Wilmington, DE, USA). The methods for qRT-PCR were described previously (Brooks et al., 2011). The targets for hybridization to GeneChip Mouse Exon 1.0 ST Arrays (Affymetrix, Santa Clara, CA, USA) were synthesized from 1 μg total RNA using the GeneChip Whole Transcript (WT) Sense Target Labeling Assay (Affymetrix). Hybridization, washing and scanning of GeneChips were performed according to the manufacturer's instructions (Affymetrix). Microarray data have been deposited in Gene Expression Omnibus under accession number GSE43951.

Laser capture microdissection (LCM)

Heads from E16.5 and P0.5 mice were cryoprotected by passage through increasing (6.75 to 25%) concentrations of ice-cold sucrose in 0.1 M phosphate buffer, equilibrated with a 2:1 mixture (volume:volume) of 25% sucrose:OCT Compound (Tissue-Tek) for 1 hour at 4°C, snap frozen on dry ice, and cryosectioned at −30°C. Cryosections (7 μm) were thaw-mounted onto PEN foil slides (Leica Microsystems), kept at −30°C for 10-30 minutes, fixed in ice-cold 70% ethanol for 30 seconds, rinsed in water, stained for 2 minutes in Meyer's Hematoxylin (Sigma-Aldrich), dehydrated through a 70-95-100% ethanol series (30 seconds each), and air-dried for 2 minutes. Cells from NR or RPE were isolated by LCM using the Leica LMD6000 system. Tissue fragments were collected by gravity into tube caps containing lysis buffer for DNA isolation.

Bisulfite pyrosequencing

Quantitation of DNA methylation was performed by bisulfite conversion followed by pyrosequencing of genomic DNA from P6.5 mouse tail and NR, or from DNA isolated from E16.5 and P0 NR and RPE using LCM. Bisulfite conversion was performed on 200 ng genomic DNA using the EZ DNA Methylation-Gold Kit (Zymo, Orange, CA, USA) following the manufacturer's protocol. After bisulfite conversion, a 20 μl PCR reaction was carried out using Hot Start Taq polymerase (Qiagen) as per manufacturer's instructions. Methylation was examined at LINE1 repeats (211 bp), in the differentially methylated region of *H19* (−3810 to −3557 bp), within exon 1 of *Opn1sw* (+25 to +226 bp), and in the 5′ UTR of *Tuba3a* (−481 to −331 bp). Primers (supplementary material Table S1) were designed using PyroMark Assay Design 2.0 software (Qiagen). PCR cycling conditions were 95°C for 15 minutes, followed by 45 cycles of 95°C for 20 seconds, 20 seconds at the annealing temperature, and 72°C for 20 seconds, with a final extension at 72°C for 5 minutes. The biotinylated PCR product was purified and made single stranded to act as a template in the pyrosequencing reaction, as recommended by the manufacturer, using the PyroMark Q24 Vacuum Prep Tool (Qiagen). Briefly, the PCR product was bound to Streptavidin Sepharose High Performance beads (Amersham Biosciences, Uppsala, Sweden) followed by purification, washing, denaturation using 0.2 M NaOH, and an additional wash. A pyrosequencing primer (0.3 μM; supplementary material Table S1) was annealed to the purified single-stranded PCR product. Pyrosequencing and methylation quantification were performed using the PyroMark Q24 Pyrosequencing System (Qiagen).

RESULTS

Dnmt1$^{fl/fl}$*:Rx-Cre/+* retinas/RPE show specific ablation of *Dnmt1* exons during development

To examine the role of DNMT1 in retinal development, we crossed homozygous mutant mice (*Dnmt1*$^{fl/fl}$, with exons 4 and 5 flanked by *loxP* sites; Fig. 1A) (Jackson-Grusby et al., 2001) with a line carrying the *Rx-Cre* transgene [*Rx*, retina and anterior neural fold

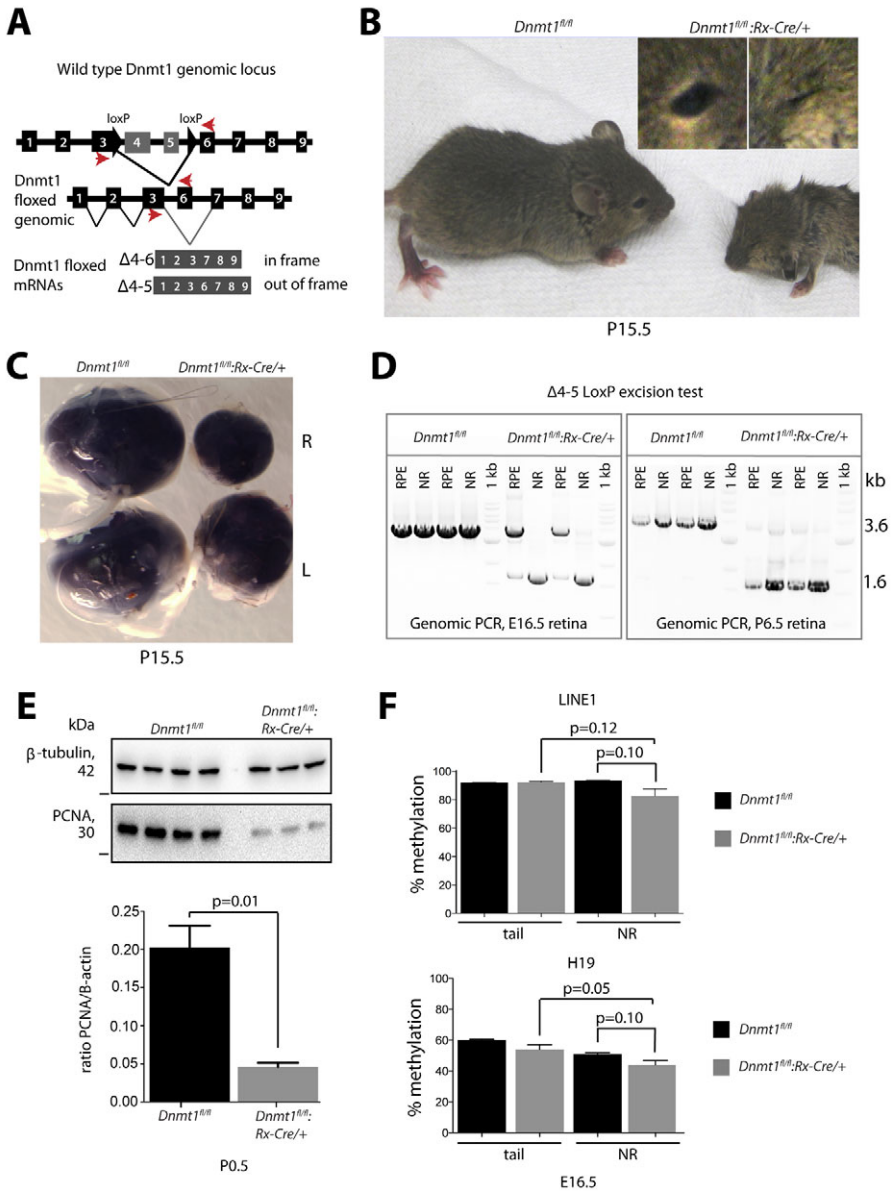

Fig. 1. Characterization of *Dnmt1*$^{fl/fl}$*:Rx-Cre/+* mutants. (**A**) Control and mutant *Dnmt1* genomic region and mutant transcripts after *Rx-Cre*-mediated excision. Red arrows represent primers used to amplify genomic DNA (exons 3-6) and cDNAs for sequencing and PCR excision. Two *Dnmt1* transcripts were detected in mutant mice: one translational out-of-frame (Δ4-5, as predicted, leading to premature truncation) and another creating an in-frame deletion (Δ4-6, due to exon 6 skipping). (**B**) P15.5 control and *Dnmt1*$^{fl/fl}$*:Rx-Cre/+* mice. The mutants are smaller and exhibit delayed eyelid opening. (**C**) The eye is smaller in mutants, with ~15% having different left (L) and right (R) eye sizes. (**D**) Excision of exons 4 and 5 occurs early in both neural retina (NR) and retinal pigment epithelium (RPE) development. (**E**) Co-immunoprecipitation of proliferating cell nuclear antigen (PCNA) with DNMT1 from P0.5 NR. (Top) Tubulin antibody staining indicates equivalent protein loading. (Middle) Immunoblot of proteins precipitated with anti-DNMT1 antibody and probed with anti-PCNA. (Bottom) There is 3-4 times less PCNA binding in the *Dnmt1* mutant. *Dnmt1* Δ4-6 preserves the DNA methyltransferase catalytic domain but lacks most of the PCNA-binding domain. (**F**) Methylation of genomic DNA in LINE1 elements and of the imprinted gene *H19* in P6.5 mutant and control NR, compared with *Dnmt1*$^{fl/fl}$ tail DNA. Average methylation of five (LINE1) or five (*H19*) CpG nucleotides is assayed in each sample; *n*=3-4 mice/assay. Error bars indicate s.e.m. *P*-values by two-tailed Student's *t*-test.

homeobox (*Rax*) – Mouse Genome Informatics] (Medina-Martinez et al., 2009), which results in specific excision of *Dnmt1* exons 4 and 5 during early development of the neural retina (NR), RPE and posterior pituitary/ventral hypothalamus (Muranishi et al., 2012). The mutant mice were runted compared with their littermate controls and had small eyes, with eyelids opening only partially (and never completely) and later than in controls (Fig. 1B,C). PCR analysis of genomic DNA from NR and RPE/choroid (RPE-Ch) samples, obtained from at least 30 control (*Dnmt1*$^{fl/fl}$) and mutant (*Dnmt1*$^{fl/fl}$*:Rx-Cre/+*) mice at different developmental stages, revealed the predicted excision of exons 4 and 5 (Jackson-Grusby et al., 2001); the excision is more efficient in NR (>95% in most animals at all ages) than in RPE-Ch (Fig. 1D), presumably because the *Rx-Cre* transgene is expressed in RPE but not in the contaminating choroidal tissue (Swindell et al., 2006) (a representative blot is shown in Fig. 1D). We noted that the choroid remained associated with RPE and could not be removed during the dissection quickly enough to avoid RNA degradation. Sequencing of RT-PCR products using primers in exon 1 and exon 9 demonstrated the presence of two *Dnmt1* transcripts in mutant retinas: one with a reported out-of-frame mutation resulting from the deletion of exons 4 and 5 (Δ4-5) (Jackson-Grusby et al., 2001) and another (Δ4-6) with an in-frame deletion due to the skipping of exon 6 during splicing (Fig. 1A; data not shown).

qRT-PCR analysis using RNA from NR and RPE-Ch revealed that *Dnmt1* expression in mutants was almost half that in controls at P0.5 and even at E14.5 (supplementary material Table S3; data not shown). As a measure of the efficiency of *Dnmt1* deletion, we performed co-immunoprecipitation with PCNA because the DNMT1 domain encoded by exons 4-6 is known to be important for PCNA binding (Spada et al., 2007); thus, the deletion event in mutant mice should lead to decreased PCNA co-immunoprecipitation. Reduced levels of DNMT1 were evident by immunoblot analysis in P0.5 mutant NR compared with control NR (data not shown). Consistent with excision, our co-immunoprecipitation analysis using NR extracts revealed a 3- to 4-fold reduction in the amount of PCNA pulled down by mutant DNMT1 compared with the wild type (Fig. 1E).

We observed a modest reduction of total DNA methylation, as measured by methylation of the LINE1 element (usually 90-100%)

and methylation of the imprinted gene *H19* (usually ~50%) in mutant NR (Fig. 1F), as indicated previously in cells carrying the in-frame Δ3-6 Cre-mediated excision (Spada et al., 2007). LINE1 methylation in control NR was 93.5±0.2% compared with 82.6±5% in mutant NR (n=3 each) with marginal significance (P=0.0951), whereas tail DNA of mutants and controls showed similar methylation (92.2±0.2% controls versus 92.4±0.6% mutants, n=3 each). *H19* methylation at six CpGs in mutant NR (43.9±2.8%, n=4) was reduced compared with control NR (50.9±0.9%, n=3) (P=0.0993). In tail DNA, *H19* methylation was similar in control and mutant samples.

Our data thus point to a knockdown of DNMT1 function (hypomorph) in *Dnmt1$^{fl/fl}$:Rx-Cre/+* mice caused by moderately reduced expression of mutant DNMT1 with an in-frame deletion of the PCNA-interacting domain.

Dnmt1$^{fl/fl}$:Rx-Cre/+ retinas show normal neurogenesis and lamination but lack photoreceptor outer segments

The *Dnmt1$^{fl/fl}$:Rx-Cre/+* mice usually died 2-4 weeks after birth, probably reflecting the secondary neuroendocrine complications due to *Rx-Cre* expression in the ventral hypothalamus/posterior pituitary (Nasonkin et al., 2004). Nonetheless, the mutant mice survived long enough to allow investigation of retinal differentiation. Histological analysis of *Dnmt1$^{fl/fl}$:Rx-Cre/+* retinas demonstrated normal lamination, but there were clearly a number of abnormalities. Retinal layers, especially the outer nuclear layer (ONL) and the inner nuclear layer (INL), showed variable thickness and were uniformly thinner than in wild-type retina (Fig. 2A). The RGC layer also displayed reduced cell numbers (Fig. 2A; supplementary material Fig. S1A), which correlated with noticeable thinning of the optic nerve (supplementary material Fig. S1B).

A key aspect of the mutant retina phenotype was consistent detachment of the NR from the RPE at E16.5 (Fig. 2A, arrows), or even earlier at E12.5-14.5. Indeed, poor adhesion between the NR and RPE in the mutant, but not in the control, eyes provided a robust way to sort the mutant and control mice even before genotyping. Additional electron microscopy (EM) studies demonstrated the absence of photoreceptor OSs in P15.5 mutant retina (Fig. 2B,C) and poorly developed microvilli in the RPE (Fig. 2C, arrowheads). Only mitochondria-rich inner segments could be observed in between photoreceptor nuclei and the RPE (Fig. 2C, asterisks).

Altered chromatin patterns in ONL and INL of mutant retina and mislocalization of DNMT1

As DNMT1 can modulate chromatin conformation (Jaenisch and Bird, 2003), we explored the chromatin patterns in mutant retina using antibodies against heterochromatin- and euchromatin-specific histone modifications (H4K20Me3 and H3K4Me3, respectively). The *Dnmt1$^{fl/fl}$:Rx-Cre/+* retina showed significant and consistent changes in the typical heterochromatin, and to a lesser extent euchromatin, staining patterns in the ONL and INL (Fig. 3A). Specifically, distinct rod- and cone-specific heterochromatin patterns observed in control mouse retina (Carter-Dawson and LaVail, 1979; Nasonkin et al., 2011) were not apparent, and the typical strong nuclear heterochromatin-specific signal was absent in the outer half of the INL layer (Fig. 3A). The DNMT1 staining that colocalized with the euchromatin marker H3K4Me3 in control cone photoreceptors (Nasonkin et al., 2011) was undetectable in most P15.5 mutant retinas (Fig. 3B), pointing to a likely change in chromatin conformation. Mutant RPE did not exhibit major changes in heterochromatin and euchromatin staining patterns within the nuclei, even though the cells were abnormal (Fig. 3B).

All cell types except S-cones are present in *Dnmt1* mutant retina

To evaluate the effect of *Dnmt1* knockdown on retinal cell fate, we performed high-resolution confocal microscopy using antibodies

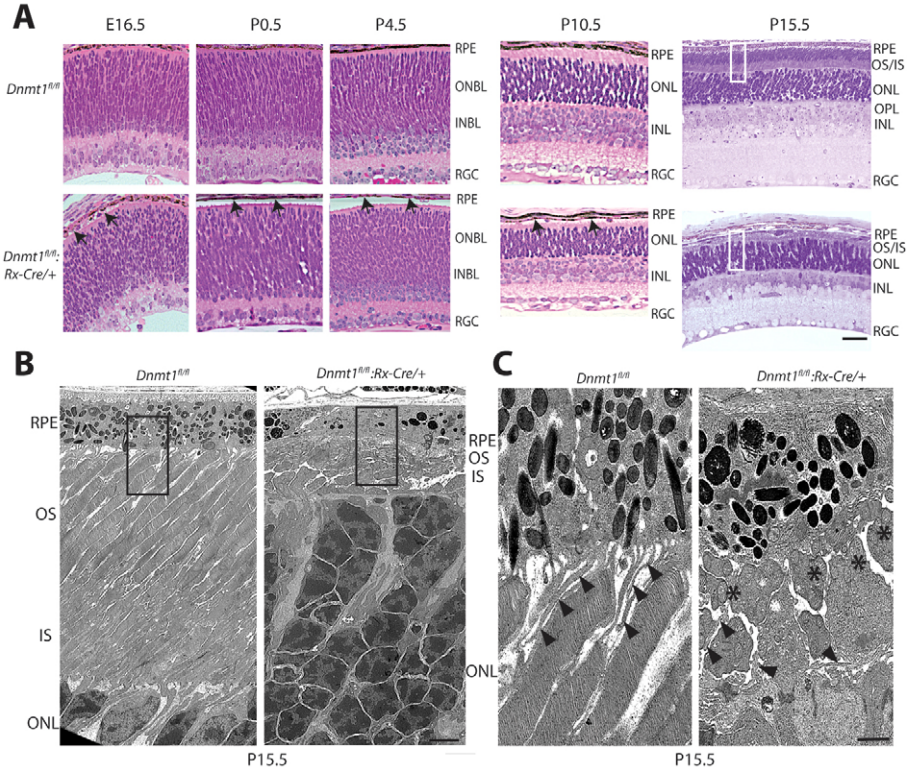

Fig. 2. Thin retinal layers and absence of photoreceptor outer segments in *Dnmt1$^{fl/fl}$:Rx-Cre/+* mice. (**A**) Retinal histology (H&E staining) in mutant and control retinas. Mutants display normal retinal lamination and reduced RPE/NR adhesion from E16.5 (arrows). At P8.5-P10.5, the ONL and INL become progressively thinner; the RGC layer shows fewer cells. By P15.5, mutant retinas show no photoreceptor OS and a disorganized, partially depolarized RPE cell layer with enlarged melanin granules. (**B**,**C**) P15.5 NR/RPE junction by EM at 3000× and 10,000× magnification, respectively, showing lack of photoreceptor OS and disorganized inner segments with aggregated mitochondria (asterisks) in mutant retinas; the presence of mitochondria between photoreceptor nuclei and RPE confirms the absence of OS. RPE microvilli (arrowheads) are disorganized in mutant retina. RPE, retinal pigment epithelium; ONBL, outer neuroblastic layer; INBL, inner neuroblastic layer; ONL, outer nuclear layer; INL, inner nuclear layer; RGC, retinal ganglion cell layer; OS, outer segment; IS, inner segment. Boxes in A and B indicate the photoreceptor/RPE junction area. Scale bars: 50 μm in A; 2 μm in B; 500 nm in C.

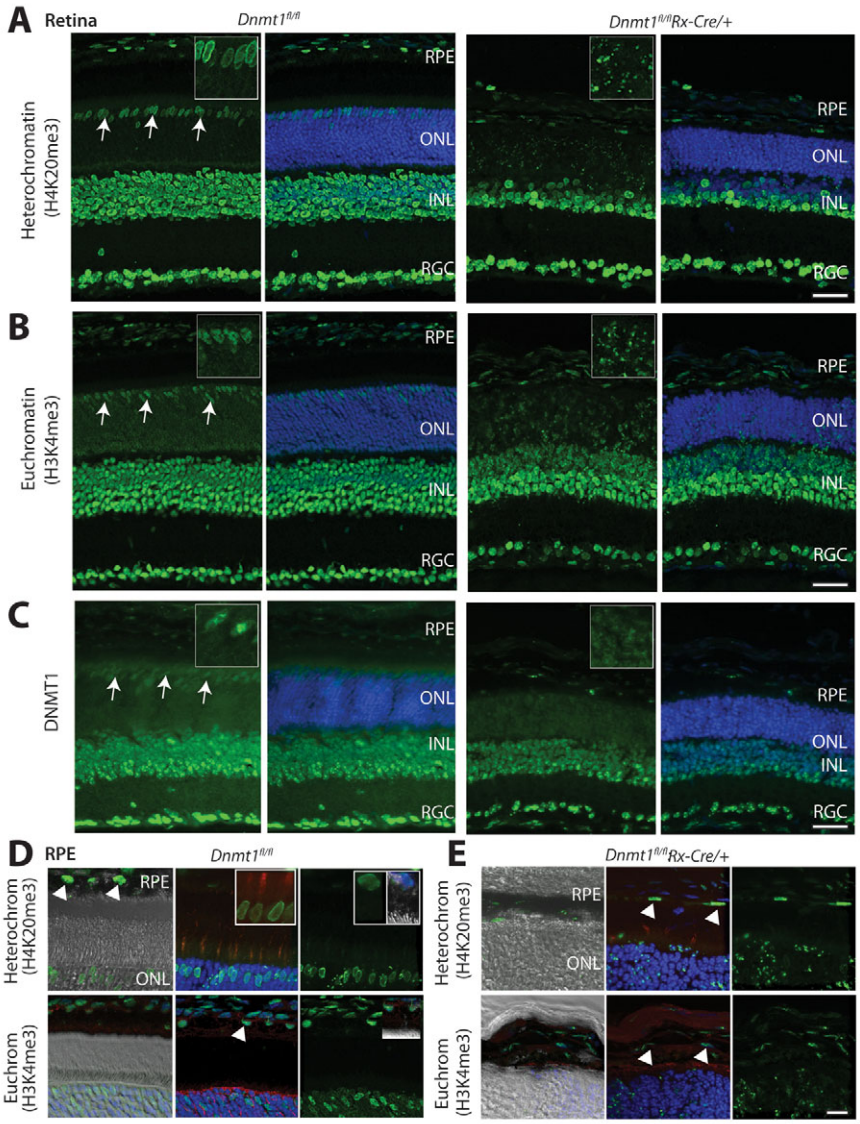

Fig. 3. Altered distribution of heterochromatin, euchromatin and DNMT1 in *Dnmt1* mutant retina. P15.5 cryosections immunostained with antibodies to heterochromatin marker H4K20me3 (A,D,E), euchromatin marker H3K4me3 (B,D,E) and DNMT1 (C). Nuclei are DAPI counterstained (blue). (**A**,**B**) Dramatic changes in heterochromatin and euchromatin distribution in the mutant ONL, especially in cones. Insets show an enlarged image of the ONL. Distinct cone chromatin patterns (arrows) are lacking in mutants, although cones are still present (red PNA staining, E; compare with D, top middle panel). (**C**) DNMT1 distribution in mutant retina lacks the typical cone nuclear staining (arrows). (**D**,**E**) Confocal images of heterochromatin and euchromatin (green) in control (D) and mutant (E) retina. Left panels, differential interference contrast (DIC) and chromatin staining (green); middle top panels, PNA staining of cone IS/OS (red) with DAPI (blue) and chromatin staining; right panels, chromatin staining only. (D) Inset, middle: H4K20me3 nuclear staining is cone specific, as red (PNA) and green (chromatin) originate from the same cells. (D) Inset, top right: strong nuclear H4K20me3 staining in control RPE. (D,E) Middle lower panels: the Müller glia marker glutamine synthetase (red) with DAPI and euchromatin staining. Euchromatin and heterochromatin patterns are preserved in mutant RPE regardless of changes in RPE polarity (flat and disorganized RPE cells, arrowheads). RPE, retinal pigment epithelium; ONL, outer nuclear layer; INL, inner nuclear layer; RGC, retinal ganglion cell layer. Scale bars: 50 μm in A-C; 20 μm in D,E.

that identify distinct cell types. Immunostaining for photoreceptor-specific markers – rhodopsin, PRPH2 and recoverin – revealed their near normal expression in inner segments (Fig. 4A,B; supplementary material Fig. S2) of *Dnmt1*$^{fl/fl}$*:Rx-Cre/+* retina, even though OSs were absent (see Fig. 2). Surprisingly, there was a significant underrepresentation of cones in P15.5 mutant retina as shown by peanut agglutinin (PNA) staining (Fig. 4B,C), a reduced number of M-cones as measured by M-opsin antibody (Fig. 4B), and a complete absence of S-opsin immunostaining (Fig. 4B). In concordance, *Opn1sw* (S-opsin) RNA expression was reduced by at least 50% in mutant retina as assessed by qRT-PCR analysis (Fig. 4D).

We investigated whether altered neuroendocrine function in *Dnmt1*$^{fl/fl}$*:Rx-Cre/+* mice might contribute to the striking difference in M-cones and almost complete absence of S-opsin-expressing cones, as cone opsin expression is controlled by thyroid hormone in developing and mature retina (Roberts et al., 2006; Glaschke et al., 2011). We examined the cones in adult hypopituitary *Ames dwarf* (*Prop1*$^{df/df}$) mice. PNA staining (which labels both M- and S-cone matrix sheath) of the *Prop1*$^{df/df}$ retina revealed a normal density of cones (per field), as compared with age-matched wild-type littermates (supplementary material Fig. S3).

Consistent with a thinner (about half that of controls) and pallid optic nerve, the number of RGCs was reduced in *Dnmt1*$^{fl/fl}$*:Rx-Cre/+* mutants, as evidenced by BRN3A and BRN3B (POU4F1 and POU4F2 – Mouse Genome Informatics) staining at E16.5 and P0.5 (see supplementary material Fig. S1). We did not observe a significant difference in immunostaining using specific markers of other retinal cell types – ON bipolar neurons (PKCα), horizontal cells (CALB1 and PROX1), amacrine (CALB2) and Müller glia (cyclin D3 and glutamine synthetase) – in P15.5 *Dnmt1*$^{fl/fl}$*:Rx-Cre/+* retina (supplementary material Figs S4-S6; data not shown).

Gene expression in *Dnmt1*$^{fl/fl}$*:Rx-Cre/+* retina

To understand the molecular basis of NR abnormalities, specifically the lack of photoreceptor OSs, we generated expression profiles of *Dnmt1*$^{fl/fl}$ control and *Dnmt1*$^{fl/fl}$*:Rx-Cre/+* retina at different developmental stages using exon arrays (GeneChip, Affymetrix) (supplementary material Table S4). Surprisingly, we did not observe significant changes in the expression of a number of genes that encode transcription factors, phototransduction (except a few cone genes, including S-opsin) and/or cilia proteins associated with homeostasis, OS biogenesis or intracellular trafficking (e.g. *Nrl*,

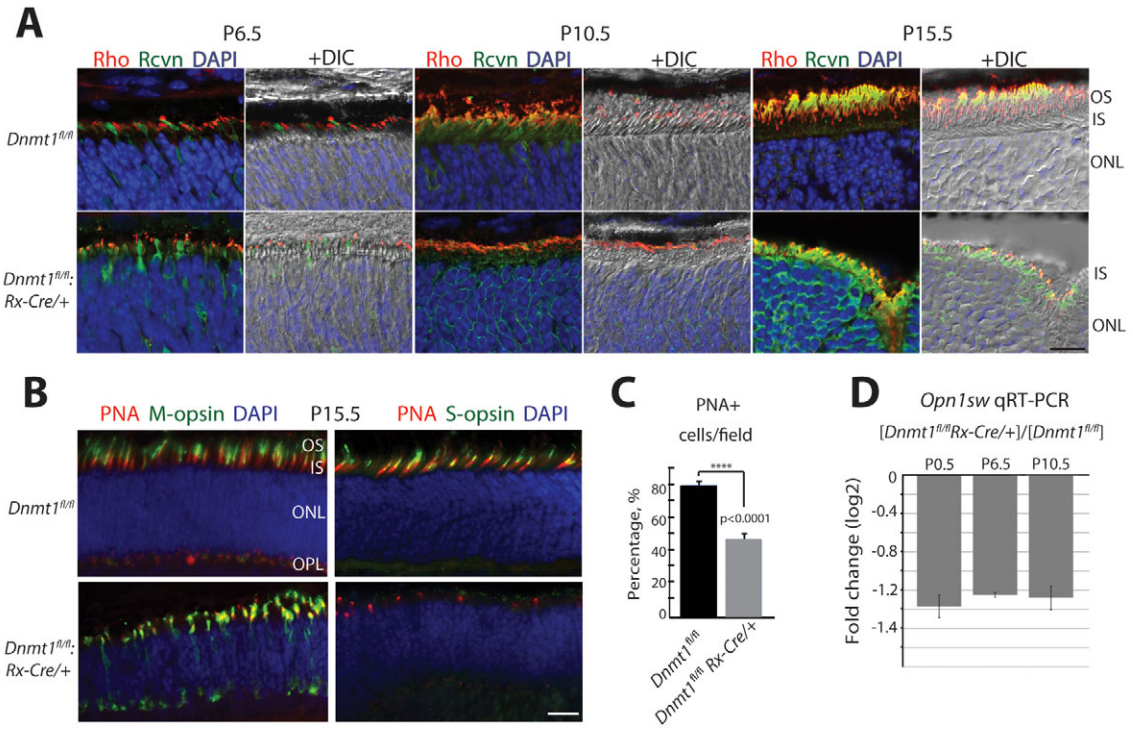

Fig. 4. Defects in photoreceptor maturation and lack of S-cones in *Dnmt1* mutant retina. (**A**) DIC and immunofluorescence images with antibodies to photoreceptor OS (rhodopsin) and IS (recoverin) in control and mutant mice. OS development is halted in mutant retinas between P6.5 and P10.5, with rhodopsin and recoverin aggregated in IS. (**B**) Immunofluorescence staining of M- and S-cones in control and mutant P15.5 retinal sections. Left panels, PNA (red) and M-opsin antibody (green); right panels, PNA (red) and S-opsin antibody (green). There is reduced PNA and M-opsin in the mutant; S-cone staining was present in control littermates (9/9) but not in mutants (0/13). (**C**) Loss of cone cells in *Dnmt1*$^{fl/fl}$*:Rx-Cre/+* retinas. *n*=5 fields counted per graph. Error bars, s.e.m. *P*-values by two-tailed *t*-test. (**D**) Quantification of *Opn1sw* (short-wave cone opsin) expression in the NR of mutants, relative to control littermates (*n*=4 per genotype, each analyzed in triplicate). Rho, rhodopsin; Rcvn, recoverin; IS, inner segment; OS, outer segment; ONL, outer nuclear layer. Scale bars: 20 μm in A; 50 μm in B.

Crx, *Mef2c*, *Esrrb*, *Nr2e3*, *Gnat1*, *Prph2*, *Rom1*, *Cnga3*, *Aipl1*, *Rpgr*, *Rpgrip1*, *Tulp1*, *Prom1*, *Mkks*, *Bbs2*, *4*, *5*, *7*, *9*) (data not shown). A diverse set of genes showed aberrant (generally higher) expression in the mutant retina at early stages of development (E16.5 and P0.5; supplementary material Tables S3, S4), a likely result of hypomethylation at distinct genomic loci. However, the expression of most genes was unaltered at later stages of photoreceptor development (e.g. at P6.5 and P10.5; supplementary material Tables S3, S4). The greatest increase in expression was detected for *Tuba3a*, the expression of which is strongly affected by methylation (Borgel et al., 2010).

RPE abnormalities in *Dnmt1*$^{fl/fl}$*:Rx-Cre/+* retina

Extensive retinal detachment, together with striking abnormalities in photoreceptors, led us to examine the RPE in *Dnmt1*$^{fl/fl}$*:Rx-Cre/+* retina. As early as E16.5, a highly disorganized RPE monolayer contained cells of variable height and pigmentation, abnormally sized nuclei and variable compaction of heterochromatin (Fig. 5A). This disorganized monolayer was particularly evident in flat-mounted RPE stained with phalloidin to decorate F-actin and with DAPI to identify nuclei (Fig. 5B). Differential interference contrast (DIC) or brightfield microscopy revealed homogeneous pigmentation of control RPE cells but variable degrees of pigmentation in mutant RPE (Fig. 5B, bottom panels).

Analysis of 3D confocal stacks demonstrated the variable position of junctional actin in mutant RPE, in striking contrast to the uniform height and position of junctional actin in control RPE (green signal; Fig. 5B, bottom; 5C, top) and less F-actin on the apical surface of mutant RPE cells, indicative of underdeveloped apical microvilli (green signal; Fig. 5C, middle). β-catenin (a lateral membrane marker) and adherens junctions were also highly disorganized in mutant RPE (red signal; Fig. 5C, bottom). Confocal imaging of P15.5 mutant and control retina vibratome sections demonstrated shorter microvilli in mutants (Fig. 5D) and a highly disorganized distribution of ezrin (green signal; Fig. 5C, bottom), a scaffolding protein that plays a key role in the development of apical microvilli and basal infoldings of RPE (Bonilha et al., 1999). In agreement, EM analysis at P15.5 revealed highly organized microvilli and basal infoldings in control RPE and poorly developed microvilli and basal infoldings in mutant RPE (Fig. 5E). Notably, labeling with antibody to rootletin (Crocc) in the RPE of *Dnmt1*$^{fl/fl}$*:Rx-Cre/+* mice identified irregular ciliary rootlets (supplementary material Fig. S7), providing further evidence of disruption of RPE organization and polarity.

Ablation of *Dnmt1* exons in RPE but not in NR results in defective photoreceptor outer segment biogenesis

To decipher the mechanism of defective photoreceptor OS biogenesis, we used different *Cre* transgenic lines to selectively knockdown *Dnmt1* in RPE and/or NR. We bred *Dnmt1*$^{fl/fl}$ mice with those expressing a doxycycline (DOX)-inducible *VMD2-Cre* transgene (Le et al., 2008), which is specifically expressed in RPE (Fig. 6A-E). The genomic PCR assay confirmed the predicted

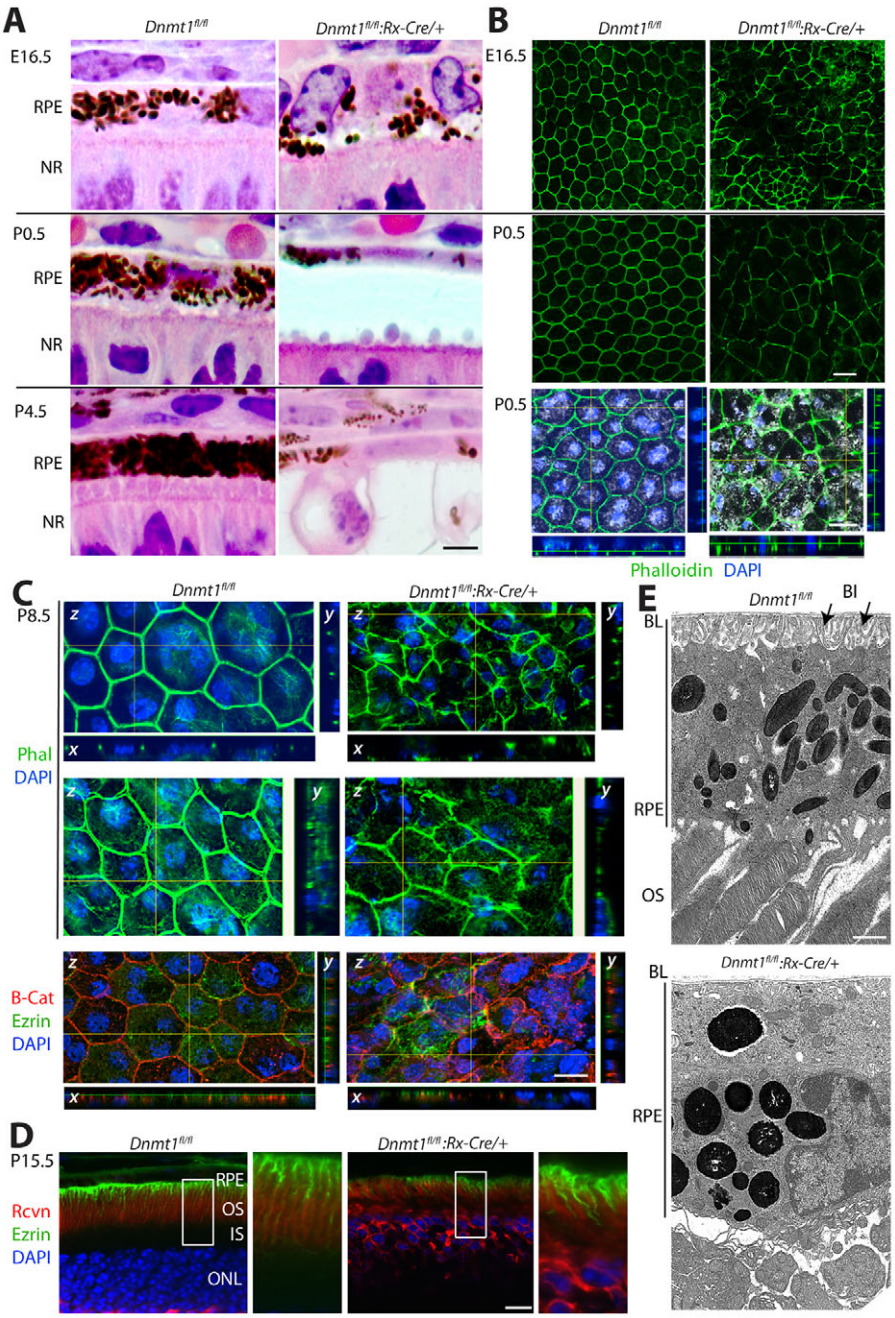

Fig. 5. Early disruption of RPE polarity in *Dnmt1* mutant retina. (**A**) H&E staining of sections of control and mutants retinas showing the RPE-NR junction. Abnormal RPE development was noted in mutants at E16.5, including poor NR/RPE adhesion, variable cell height and pigmentation, inconsistent nuclear size and variable heterochromatin compaction. (**B**) Disruption of the actin cytoskeleton in mutant RPE. Phalloidin staining (green) of filamentous actin in RPE flatmounts shows the lack of a cobblestone arrangement in the mutant RPE. Bottom panels are optical section *z*-stacks of P0.5 RPE flatmounts with DIC showing melanin distribution in RPE. *z*-stacks virtually resectioned in *x* and *y* planes reveal uniform pigmentation, cell height and position of junctional actin in control RPE, but not in mutant RPE. (**C**) Maximum projection *z*-stack images of flatmount RPE preparations at P8.5 prior to OS elongation showing staining with phalloidin (green) and for RPE polarity markers (red). *z*-stacks were virtually resectioned in the *x* and *y* planes (top panels) and compressed along the *y*-plane (middle panels). Mutant RPE shows variable cell height and position of junctional actin (top), reduced apical F-actin (middle) and disorganized apical microvilli and basal infoldings, as marked by ezrin (bottom). A similar pattern is observed for β-catenin, a lateral membrane marker. (**D**) Confocal images of vibratome sections demonstrate shorter microvilli (labeled with ezrin antibody, green) in mutant RPE. (**E**) EM of RPE (10,000×) revealed less well developed microvilli and basal infoldings (BI) in the mutant (arrows). The basal lamina (BL) appeared unaltered. Scale bars: 10 μm in A-C; 20 μm in D; 500 nm in E.

ablation of *Dnmt1* exons 4 and 5 in RPE but not in the NR of *Dnmt1*$^{fl/fl}$*:VMD2-Cre* DOX^{+} mice (Fig. 6A).

About 12% of the mutant, but not control, newborn pups demonstrated microphthalmia and RPE hypopigmentation (Fig. 6B). The eyes of mutant pups were frequently smaller (Fig. 6C). Strikingly, continuous administration of DOX in pregnant mice to excise exons 4 and 5 as early as *VMD2-Cre* transgene expression (Le et al., 2008) resulted in shortening of the OSs in *Dnmt1*$^{fl/fl}$*:VMD2-Cre* retina but not in control *Dnmt1*$^{fl/fl}$ or heterozygous retina (Fig. 6D). The dynamics of OS elongation was dependent on the efficiency of DOX-induced *VMD2-Cre* transgene activation, which can be inherently variable (Le et al., 2008). As DOX was included in the diet, the timing and extent of its effect on the OS in different mice, even within a litter, were different; yet, the defects in OS morphogenesis were clearly evident by P15.5. Mutant retina displayed areas of NR/RPE detachment as observed in *Dnmt1*$^{fl/fl}$*:Rx-Cre/+* mice (Fig. 6D, arrows). The RPE flatmount preparations also revealed a disrupted actin cytoskeleton (Fig. 6E), in accordance with the data from *Dnmt1*$^{fl/fl}$*:Rx-Cre/+* pups.

We then used *Pax6-[α]Cre* (Marquardt et al., 2001), *Six3-Cre* (Furuta et al., 2000) and *Crx-Cre* transgenes (Nishida et al., 2003) to excise *Dnmt1* exons primarily in the developing NR. We independently validated the effectiveness of *Six3-Cre* and *Crx-Cre* transgenes using the *ROSA26-lacZ* reporter (data not shown). The *Pax6-[α]Cre* mice express robust Cre activity in the retinal periphery but not in the central retina (Marquardt et al., 2001; Bäumer et al., 2002). As predicted, we observed rapid degeneration of the peripheral but not central retina in *Dnmt1*$^{fl/fl}$*:Pax6-[α]Cre/+* mice (Fig. 6F), and rapid degeneration of predominantly central NR but not RPE in *Dnmt1*$^{fl/fl}$*:Six3-Cre/+* retina (Fig. 6G). The mutant

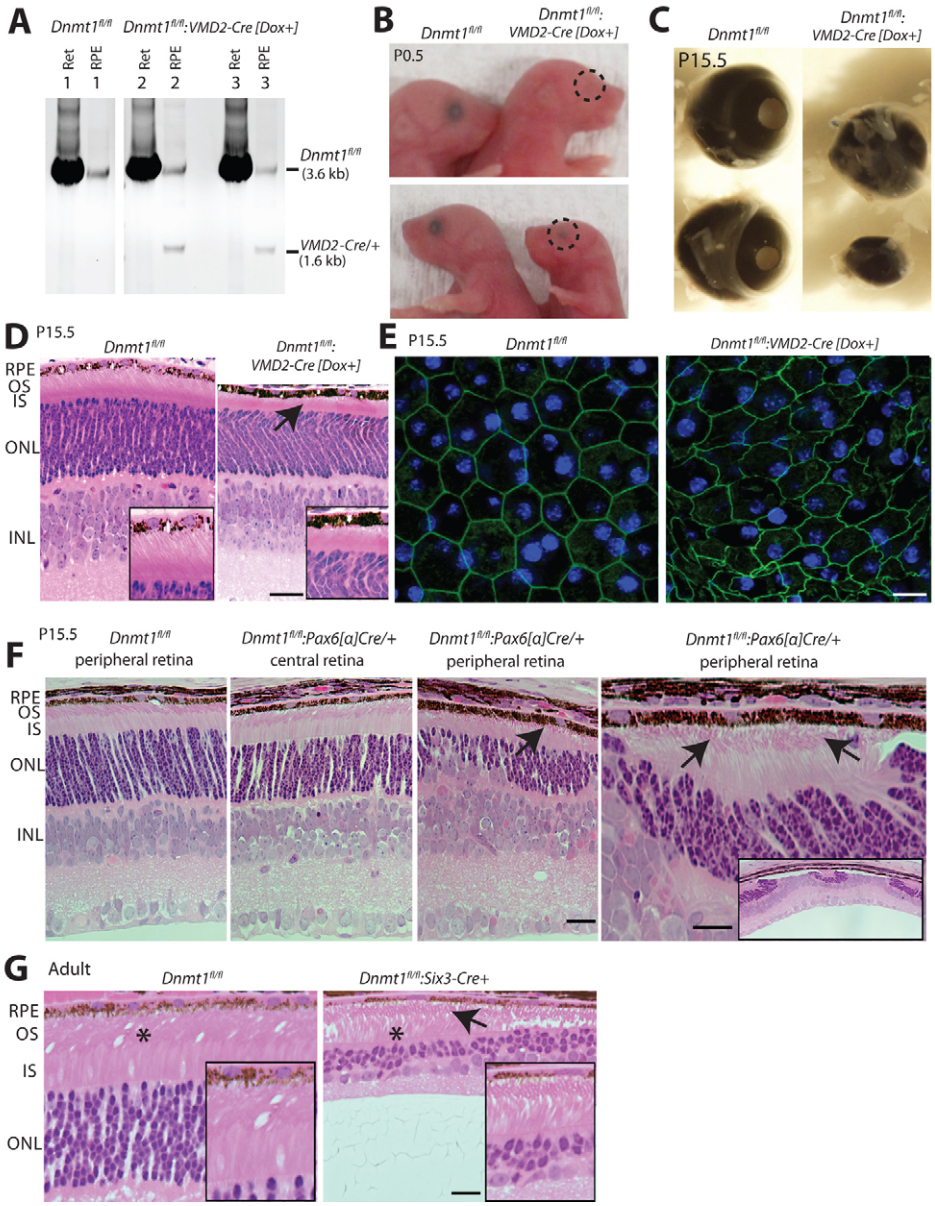

Fig. 6. RPE-specific disruption of Dnmt1 prevents photoreceptor OS elongation. (**A**) Dnmt1 Δ4-5 excision demonstrates doxycycline-induced *VMD2-Cre* transgene activity in RPE but not NR (Ret). (**B**) Microphthalmia and severe loss of RPE pigmentation in P0 *Dnmt1*$^{fl/fl}$*:VMD2-Cre* doxycycline-treated *[Dox+]* mice. (**C**) Smaller eyes in P9 *Dnmt1*$^{fl/fl}$*:VMD2-Cre [Dox+]* mice, resembling those consistently observed in the *Dnmt1*$^{fl/fl}$*:Rx-Cre/+* model. (**D**) Methacrylate sections of *Dnmt1*$^{fl/fl}$*:VMD2-Cre [Dox+]* mice and littermate controls (*Dnmt1*$^{fl/fl}$), showing loss of OS in mutant mice and signs of poor adhesion between retina and RPE in mutants (arrow). (**E**) Compressed *z*-stacks of RPE flatmounts at P9 showing phalloidin (green) with nuclear DAPI counterstain (blue). Mutant RPE shows actin cytoskeleton abnormalities resembling those in *Dnmt1*$^{fl/fl}$*:Rx-Cre/+*. (**F**) Methacrylate sections of control (*Dnmt1*$^{fl/fl}$) and *Dnmt1*$^{fl/fl}$*:Pax6-[a]Cre* littermates, in which *Dnmt1* excision takes place in the peripheral but not central NR, resulting in degeneration of peripheral NR (third panel from the left). However, OSs remain (arrows) as long as some photoreceptors are preserved in the ONL. (**G**) Likewise, in *Dnmt1*$^{fl/fl}$*:Six3-Cre* mice, OSs are preserved (arrow), despite *Dnmt1* excision in NR and significant peripheral NR degeneration (shown). Asterisks indicate the areas enlarged in the insets. Scale bars: 50 μm in D; 10 μm in E; 20 μm in F,G.

retina in both instances had normal OS elongation and RPE morphology before NR degeneration. The only phenotype displayed by *Dnmt1*$^{fl/fl}$*:Crx-Cre/+* retina was retinal degeneration that noticeably developed by P15.5 (data not shown). OSs, however, elaborated normally.

Altered expression of selected signaling genes in mutant RPE-choroid

Based on the gene profiling data (supplementary material Table S4), we selected 75 genes that might impact photoreceptor differentiation and/or maturation and performed qRT-PCR analysis in control and mutant RPE-Ch (supplementary material Table S5). We observed a substantial reduction in the expression of *Ihh* [which is expressed in choroid (Dakubo et al., 2008)] at P0.5 (5.2-fold) and P6.5 (3.3-fold), *Ptch2* (2.2-times less at P0.5 and 2.3-times less at P6.5), *Wnt3a* (1.5-times less at P6.5) and *Sfrp5* (2-times less at P0.5). The expression of two Notch pathway genes, *Hes1* and *Dll1*, was also more than halved at P0.5 and P6.5, whereas *Fzd5* expression was increased by 2.3-fold at P0.5. Notably, high expression of *Tuba3a* was detected at E14.5 (80-fold) and P6.5 (132-fold). However, a majority of early RPE development genes showed no significant change in expression in qRT-PCR analysis using the criteria of fold change ≥2.0 with $P \leq 0.05$ in a set of four biological replicates at each time point and for each genotype (*Dnmt1*$^{fl/fl}$ and *Dnmt1*$^{fl/fl}$*:Rx-Cre/+*).

DNA methylation in mutant NR and RPE

To elucidate how *Dnmt1* knockdown affected NR versus RPE methylation and consequently photoreceptor development, we examined global DNA methylation [LINE1 elements (Poage et al., 2011)] and the methylation of two genes, *Tuba3a* and *Opn1sw*, that exhibited significantly altered expression in *Dnmt1*$^{fl/fl}$*:Rx-Cre/+* mutant retina (Fig. 7). For LINE1 and *Tuba3a*, genomic DNA was isolated from NR and RPE, obtained by laser capture microdissection (LCM) from E16.5 and P0.5 retina of control and mutant mice, and used for pyrosequencing (Ronaghi et al., 1998). A significantly greater reduction in global DNA methylation was detected in mutant RPE as compared with mutant NR (Fig. 7A). Methylation of *Tuba3a*, which showed dramatically higher

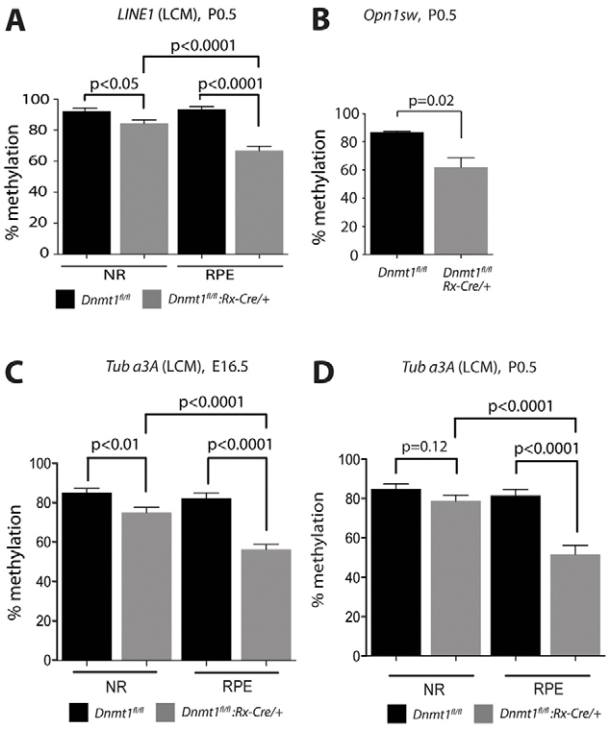

Fig. 7. Change in DNA methylation in *Dnmt1*$^{fl/fl}$*:Rx-Cre/+* NR and RPE. (**A**) DNA methylation in P0.5 control and mutant RPE and NR (n=3-4 for each cohort), isolated by laser capture microdissection (LCM). The five CpG sites in LINE1 that were analyzed in each sample showed more pronounced demethylation in mutant RPE than in mutant NR. A similar trend was found at E16.5 (not shown). (**B**) Quantification of *Opn1sw* promoter methylation at P0.5 (n=3), measured in NR using bisulfite pyrosequencing; methylation data from three CpG sites were averaged. (**C**,**D**) Demethylation of the proximal *Tuba3a* promoter in NR and RPE of mutant mice. Shown is the average methylation of five CpG sites in the *Tuba3a* promoter obtained from DNA of LCM samples of NR and RPE at E16.5 (C) and P0.5 (D) of control and mutant mice (n=3-4). Error bars, s.e.m. *P*-values by two-tailed Student's *t*-test.

expression in both mutant RPE and NR by qRT-PCR, was reduced in mutants compared with controls at five CpG sites located near the transcription start site; however, RPE exhibited more pronounced demethylation than NR (Fig. 7C,D). Our results imply a direct effect of hypomethylation at the locus on *Tuba3a* transcription.

Pyrosequencing of three CpG sites at *Opn1sw* (S-opsin, expressed in S-cones) using P0.5 NR genomic DNA identified a substantial decrease in methylation in mutants (61.9±6.8% versus 87.0±0.6% in controls, n=5; Fig. 7B). Reduced CpG methylation, yet decreased expression of S-opsin, in the mutant retina (see Fig. 4D) suggests an indirect effect via concurrent demethylation at an unidentified suppressor of *Opn1sw*.

DISCUSSION

Here, we report for the first time that *Dnmt1* knockdown in RPE, but not in NR, results in specific changes in RPE structure, and possibly function, and is associated with aberrant photoreceptor development and lack of OS morphogenesis. The complete absence of OSs is not due to major changes in the expression of phototransduction or cilia transport genes. Yet, reduced DNMT1 function in early retinal development does not affect cell type specification and lamination. Consistent with our findings, a recently reported NR-specific knockdown of *Dnmt1* using a *Chx10-Cre* driver (*Chx10* is also known as *Vsx2* – Mouse Genome Informatics) revealed the generation of all classes of retinal cell types; however, this mutant exhibited abnormal expression of rhodopsin and M-opsin and a progressive loss of all nuclear layers (Rhee et al., 2012). In addition to revealing a novel role of RPE in photoreceptor maturation, our *Dnmt1* knockdown mutants provide useful models with which to dissect the epigenetic control mechanisms and signaling molecules that guide the differentiation of the photoreceptor-RPE interface.

Epigenetic reprogramming is established in early stages of development, and recent studies indicate a continuous dynamic control of the epigenome (Branco et al., 2008; Illingworth et al., 2008; Wu and Zhang, 2011; Yaish et al., 2011). DNMT1 is primarily responsible for maintaining DNA methylation and is necessary for survival; however, its interaction with PCNA does not appear to be crucial for enzymatic function (Egger et al., 2006; Chen et al., 2007; Spada et al., 2007; Hirasawa et al., 2008). Interestingly, the loss of the PCNA-binding domain in the *Dnmt1* knockdown mutant reported here did not broadly impact eye development, acquisition of NR and RPE cell fate or gene expression patterns. Nonetheless, subtle changes in the expression of genes in the differentiating RPE-Ch can be associated with altered cell shape, size and polarity. Of specific importance are alterations in several signaling molecules and transcription factors, including *Bmp2*, *Bmp4*, *Fzd5*, *Hes1*, *Ihh*, *Mitf*, *Ptch2* and *Sfrp5*. Further investigations are necessary to delineate their precise roles in RPE development.

The genesis of OSs that include the complete machinery for phototransduction is a hallmark of ciliated photoreceptors and is initiated at ~P9 in mice. The relatively small changes in the expression of photoreceptor genes that we observed seems unlikely to account for RPE detachment and the complete absence of OSs in the *Dnmt1* mutant mice. We were intrigued by a possible direct link between RPE integrity and photoreceptor differentiation, as reflected in the phenotypes of the various *Dnmt1* mutants created with RPE and/or NR-Cre lines. RPE secretes a many chemokines and cytokines (Shi et al., 2008); however, our data also suggest a key role for cell-cell interaction in producing the requisite inductive signals for OS biogenesis.

The expression of mutant *Dnmt1* resulted in small mice with variably small eyes. The small size of the mice could be due to hormonal insufficiency (Nasonkin et al., 2004) resulting from *Rx-Cre* activity in the ventral hypothalamus/posterior pituitary in addition to the developing eye (Swindell et al., 2006; Medina-Martinez et al., 2009). However, the small eye phenotype of *Dnmt1*$^{fl/fl}$*:Rx-Cre/+* mice is likely to be a consequence of the expression of mutant *Dnmt1* in the NR and RPE rather than a result of hypothalamic insufficiency, as hypopituitary *Prop1*$^{df/df}$ mice have normal sized eyes (data not shown) and a normal rod:cone ratio (supplementary material Fig. S3).

Our studies suggest an instructive function of RPE in the biogenesis of photoreceptor OSs, which are elaborated from a uniquely modified primary cilium (Liu et al., 2007). The primary cilium in RPE develops early, but disappears once the retina is mature (Nishiyama et al., 2002). In the adult, RPE microvilli are in close contact with photoreceptors. We hypothesize that if the RPE cilium or associated signaling is disrupted, it could prevent photoreceptor OS biogenesis. Disorganization of ciliary rootlets (supplementary material Fig. S7) and reduced *Ihh* expression in postnatal RPE-Ch, as observed in *Dnmt1*$^{fl/fl}$*:Rx-Cre/+* mice, might indicate defective signaling through the RPE cilium. Misregulation of *Ihh* has been linked to aberrant photoreceptor development (Dakubo et al., 2008).

Significant overexpression of *Tuba3a*, a microtubule protein present in primary cilia (Arikawa and Williams, 1993), in mutant NR and RPE is consistent with this hypothesis. The *Tuba3a* promoter in NR and RPE indeed showed a significant decrease in proximal promoter methylation, in agreement with the drastic upregulation of *Tuba3a* expression. Additionally, we observed expression changes in cilia-associated genes in both NR and RPE and in signaling molecules that might control RPE polarization (Ihh, Wnt/Frizzled pathways). Hence, misregulation of cilia formation in RPE might be a contributing factor to altered RPE-photoreceptor interaction during postnatal retinal development.

To our surprise, statistically significant gene expression changes in the NR and RPE of mutants were limited to a few genes, including *Ihh*, *Tuba3a*, *Opn1sw* and *Dnmt1* itself (supplementary material Tables S3-S5). We believe that a single cause-effect mechanism for the failure of OS elongation is unlikely. Instead, epigenetic (DNA methylation) mechanisms tightly modulate the expression of a number of key NR and RPE genes, and these expression changes cumulatively lead to a pronounced retinal phenotype associated with the lack of photoreceptor OSs. Our findings are consistent with reports of *DNMT1* mutations that are likely to affect hearing and neurological phenotypes via pleiotropic mechanisms (Klein et al., 2011; Winkelmann et al., 2012).

Our studies have translational implications for cell-based therapies of retinal degenerative diseases. The photoreceptors produced from embryonic or induced pluripotent stem cells do not generate OSs, which are crucial for phototransduction (Osakada et al., 2008; Meyer et al., 2009). In an *in vitro* three-dimensional model that self-organized into laminated retina from embryonic stem cell aggregates, no photoreceptor OSs were observed (Eiraku et al., 2011), probably because RPE was removed before culturing the optic vesicle. Interestingly, when early (embryonic weeks 8-17) human fetal retina or mouse photoreceptor precursors are transplanted into the subretinal space immediately next to the RPE layer, such grafts undergo lamination and graft-derived photoreceptors show well-developed OSs (Sagdullaev et al., 2003; MacLaren et al., 2006; Lamba et al., 2009). The availability of stem cell-derived RPE (Klimanskaya et al., 2004; Idelson et al., 2009; Salero et al., 2012) and efficient culture protocols for polarized RPE (Sonoda et al., 2009; Bharti et al., 2011) will allow us to test whether developing and/or mature RPE is needed for photoreceptor differentiation. The identification of RPE-derived signals that instruct developing photoreceptors to produce OSs will greatly assist the design of treatment paradigms for neurodegenerative diseases involving photoreceptor dysfunction or death.

Acknowledgements
We thank Rudolf Jaenisch for *Dnmt1*$^{fl/fl}$, Guillermo Oliver for *Six3-Cre*, Peter Gruss for *[α]Cre* and Michael Masternak for Ames *Prop1*$^{df/df}$ mice; and Tiansen Li, Chi-Chao Chan, Mary Alice Crawford, Tudor Badea, Harsha Rajasimha and Dustin Hambright for assistance and advice.

Funding
This research was supported by Intramural Research Program of the National Eye Institute, National Institutes of Health [grants EY08538, EY020900, EY009769, P20RR024215 and P30EY001765]; and by The Foundation Fighting Blindness and Research to Prevent Blindness. Deposited in PMC for release after 12 months.

Competing interests statement
The authors declare no competing financial interests.

Supplementary material
Supplementary material available online at
http://dev.biologists.org/lookup/suppl/doi:10.1242/dev.086603/-/DC1

References

Arikawa, K. and Williams, D. S. (1993). Acetylated alpha-tubulin in the connecting cilium of developing rat photoreceptors. *Invest. Ophthalmol. Vis. Sci.* **34**, 2145-2149.
Bandyopadhyay, M. and Rohrer, B. (2010). Photoreceptor structure and function is maintained in organotypic cultures of mouse retinas. *Mol. Vis.* **16**, 1178-1185.
Bäumer, N., Marquardt, T., Stoykova, A., Ashery-Padan, R., Chowdhury, K. and Gruss, P. (2002). Pax6 is required for establishing naso-temporal and dorsal characteristics of the optic vesicle. *Development* **129**, 4535-4545.
Bernstein, B. E., Meissner, A. and Lander, E. S. (2007). The mammalian epigenome. *Cell* **128**, 669-681.
Besharse, J. C., Hollyfield, J. G. and Rayborn, M. E. (1977). Turnover of rod photoreceptor outer segments. II. Membrane addition and loss in relationship to light. *J. Cell Biol.* **75**, 507-527.
Bharti, K., Nguyen, M. T., Skuntz, S., Bertuzzi, S. and Arnheiter, H. (2006). The other pigment cell: specification and development of the pigmented epithelium of the vertebrate eye. *Pigment Cell Res.* **19**, 380-394.
Bharti, K., Miller, S. S. and Arnheiter, H. (2011). The new paradigm: retinal pigment epithelium cells generated from embryonic or induced pluripotent stem cells. *Pigment Cell Melanoma Res.* **24**, 21-34.
Bok, D. (1993). The retinal pigment epithelium: a versatile partner in vision. *J. Cell Sci. Suppl.* **17**, 189-195.
Bonilha, V. L., Finnemann, S. C. and Rodriguez-Boulan, E. (1999). Ezrin promotes morphogenesis of apical microvilli and basal infoldings in retinal pigment epithelium. *J. Cell Biol.* **147**, 1533-1548.
Borgel, J., Guibert, S., Li, Y., Chiba, H., Schübeler, D., Sasaki, H., Forné, T. and Weber, M. (2010). Targets and dynamics of promoter DNA methylation during early mouse development. *Nat. Genet.* **42**, 1093-1100.
Bramall, A. N., Wright, A. F., Jacobson, S. G. and McInnes, R. R. (2010). The genomic, biochemical, and cellular responses of the retina in inherited photoreceptor degenerations and prospects for the treatment of these disorders. *Annu. Rev. Neurosci.* **33**, 441-472.
Branco, M. R., Oda, M. and Reik, W. (2008). Safeguarding parental identity: Dnmt1 maintains imprints during epigenetic reprogramming in early embryogenesis. *Genes Dev.* **22**, 1567-1571.
Brooks, M. J., Rajasimha, H. K., Roger, J. E. and Swaroop, A. (2011). Next-generation sequencing facilitates quantitative analysis of wild-type and Nrl(-/-) retinal transcriptomes. *Mol. Vis.* **17**, 3034-3054.
Bumsted, K. M., Rizzolo, L. J. and Barnstable, C. J. (2001). Defects in the MITF(mi/mi) apical surface are associated with a failure of outer segment elongation. *Exp. Eye Res.* **73**, 383-392.
Carter-Dawson, L. D. and LaVail, M. M. (1979). Rods and cones in the mouse retina. I. Structural analysis using light and electron microscopy. *J. Comp. Neurol.* **188**, 245-262.
Chen, T., Hevi, S., Gay, F., Tsujimoto, N., He, T., Zhang, B., Ueda, Y. and Li, E. (2007). Complete inactivation of DNMT1 leads to mitotic catastrophe in human cancer cells. *Nat. Genet.* **39**, 391-396.
Chow, R. L. and Lang, R. A. (2001). Early eye development in vertebrates. *Annu. Rev. Cell Dev. Biol.* **17**, 255-296.
Corbo, J. C., Lawrence, K. A., Karlstetter, M., Myers, C. A., Abdelaziz, M., Dirkes, W., Weigelt, K., Seifert, M., Benes, V., Fritsche, L. G. et al. (2010). CRX ChIP-seq reveals the cis-regulatory architecture of mouse photoreceptors. *Genome Res.* **20**, 1512-1525.
Cvekl, A. and Mitton, K. P. (2010). Epigenetic regulatory mechanisms in vertebrate eye development and disease. *Heredity* **105**, 135-151.
D'Aiuto, L., Di Maio, R., Mohan, K. N., Minervini, C., Saporiti, F., Soreca, I., Greenamyre, J. T. and Chaillet, J. R. (2011). Mouse ES cells overexpressing DNMT1 produce abnormal neurons with upregulated NMDA/NR1 subunit. *Differentiation* **82**, 9-17.
Dakubo, G. D., Mazerolle, C., Furimsky, M., Yu, C., St-Jacques, B., McMahon, A. P. and Wallace, V. A. (2008). Indian hedgehog signaling from endothelial cells is required for sclera and retinal pigment epithelium development in the mouse eye. *Dev. Biol.* **320**, 242-255.
Egger, G., Jeong, S., Escobar, S. G., Cortez, C. C., Li, T. W., Saito, Y., Yoo, C. B., Jones, P. A. and Liang, G. (2006). Identification of DNMT1 (DNA methyltransferase 1) hypomorphs in somatic knockouts suggests an essential role for DNMT1 in cell survival. *Proc. Natl. Acad. Sci. USA* **103**, 14080-14085.
Eiraku, M., Takata, N., Ishibashi, H., Kawada, M., Sakakura, E., Okuda, S., Sekiguchi, K., Adachi, T. and Sasai, Y. (2011). Self-organizing optic-cup morphogenesis in three-dimensional culture. *Nature* **472**, 51-56.
Fariss, R. N., Anderson, D. H. and Fisher, S. K. (1990). Comparison of photoreceptor-specific matrix domains in the cat and monkey retinas. *Exp. Eye Res.* **51**, 473-485.
Fuhrmann, S. (2010). Eye morphogenesis and patterning of the optic vesicle. *Curr. Top. Dev. Biol.* **93**, 61-84.
Furuta, Y., Lagutin, O., Hogan, B. L. and Oliver, G. C. (2000). Retina- and ventral forebrain-specific Cre recombinase activity in transgenic mice. *Genesis* **26**, 130-132.

Glaschke, A., Weiland, J., Del Turco, D., Steiner, M., Peichl, L. and Glösmann, M. (2011). Thyroid hormone controls cone opsin expression in the retina of adult rodents. *J. Neurosci.* **31**, 4844-4851.
Hao, H., Tummala, P., Guzman, E., Mali, R. S., Gregorski, J., Swaroop, A. and Mitton, K. P. (2011). The transcription factor neural retina leucine zipper (NRL) controls photoreceptor-specific expression of myocyte enhancer factor Mef2c from an alternative promoter. *J. Biol. Chem.* **286**, 34893-34902.
Hao, H., Kim, D. S., Klocke, B., Johnson, K. R., Cui, K., Gotoh, N., Zang, C., Gregorski, J., Gieser, L., Peng, W. et al. (2012). Transcriptional regulation of rod photoreceptor homeostasis revealed by in vivo NRL targetome analysis. *PLoS Genet.* **8**, e1002649.
Hirasawa, R., Chiba, H., Kaneda, M., Tajima, S., Li, E., Jaenisch, R. and Sasaki, H. (2008). Maternal and zygotic Dnmt1 are necessary and sufficient for the maintenance of DNA methylation imprints during preimplantation development. *Genes Dev.* **22**, 1607-1616.
Hu, J., Wan, J., Hackler, L., Jr, Zack, D. J. and Qian, J. (2010). Computational analysis of tissue-specific gene networks: application to murine retinal functional studies. *Bioinformatics* **26**, 2289-2297.
Hutnick, L. K., Golshani, P., Namihira, M., Xue, Z., Matynia, A., Yang, X. W., Silva, A. J., Schweizer, F. E. and Fan, G. (2009). DNA hypomethylation restricted to the murine forebrain induces cortical degeneration and impairs postnatal neuronal maturation. *Hum. Mol. Genet.* **18**, 2875-2888.
Hwang, W., Hackler, L., Jr, Wu, G., Ji, H., Zack, D. J. and Qian, J. (2012). Dynamics of regulatory networks in the developing mouse retina. *PLoS ONE* **7**, e46521.
Idelson, M., Alper, R., Obolensky, A., Ben-Shushan, E., Hemo, I., Yachimovich-Cohen, N., Khaner, H., Smith, Y., Wiser, O., Gropp, M. et al. (2009). Directed differentiation of human embryonic stem cells into functional retinal pigment epithelium cells. *Cell Stem Cell* **5**, 396-408.
Illingworth, R., Kerr, A., Desousa, D., Jørgensen, H., Ellis, P., Stalker, J., Jackson, D., Clee, C., Plumb, R., Rogers, J. et al. (2008). A novel CpG island set identifies tissue-specific methylation at developmental gene loci. *PLoS Biol.* **6**, e22.
Jackson, G. R., Owsley, C. and Curcio, C. A. (2002). Photoreceptor degeneration and dysfunction in aging and age-related maculopathy. *Ageing Res. Rev.* **1**, 381-396.
Jackson-Grusby, L., Beard, C., Possemato, R., Tudor, M., Fambrough, D., Csankovszki, G., Dausman, J., Lee, P., Wilson, C., Lander, E. et al. (2001). Loss of genomic methylation causes p53-dependent apoptosis and epigenetic deregulation. *Nat. Genet.* **27**, 31-39.
Jaenisch, R. and Bird, A. (2003). Epigenetic regulation of gene expression: how the genome integrates intrinsic and environmental signals. *Nat. Genet.* **33 Suppl.**, 245-254.
Klein, C. J., Botuyan, M. V., Wu, Y., Ward, C. J., Nicholson, G. A., Hammans, S., Hojo, K., Yamanishi, H., Karpf, A. R., Wallace, D. C. et al. (2011). Mutations in DNMT1 cause hereditary sensory neuropathy with dementia and hearing loss. *Nat. Genet.* **43**, 595-600.
Klimanskaya, I., Hipp, J., Rezai, K. A., West, M., Atala, A. and Lanza, R. (2004). Derivation and comparative assessment of retinal pigment epithelium from human embryonic stem cells using transcriptomics. *Cloning Stem Cells* **6**, 217-245.
Lamb, T. D., Collin, S. P. and Pugh, E. N., Jr (2007). Evolution of the vertebrate eye: opsins, photoreceptors, retina and eye cup. *Nat. Rev. Neurosci.* **8**, 960-976.
Lamba, D. A., Gust, J. and Reh, T. A. (2009). Transplantation of human embryonic stem cell-derived photoreceptors restores some visual function in Crx-deficient mice. *Cell Stem Cell* **4**, 73-79.
Le, Y. Z., Zheng, W., Rao, P. C., Zheng, L., Anderson, R. E., Esumi, N., Zack, D. J. and Zhu, M. (2008). Inducible expression of cre recombinase in the retinal pigmented epithelium. *Invest. Ophthalmol. Vis. Sci.* **49**, 1248-1253.
Li, E., Bestor, T. H. and Jaenisch, R. (1992). Targeted mutation of the DNA methyltransferase gene results in embryonic lethality. *Cell* **69**, 915-926.
Liu, Q., Tan, G., Levenkova, N., Li, T., Pugh, E. N., Jr, Rux, J. J., Speicher, D. W. and Pierce, E. A. (2007). The proteome of the mouse photoreceptor sensory cilium complex. *Mol. Cell. Proteomics* **6**, 1299-1317.
Livesey, F. J. and Cepko, C. L. (2001). Vertebrate neural cell-fate determination: lessons from the retina. *Nat. Rev. Neurosci.* **2**, 109-118.
Longbottom, R., Fruttiger, M., Douglas, R. H., Martinez-Barbera, J. P., Greenwood, J. and Moss, S. E. (2009). Genetic ablation of retinal pigment epithelial cells reveals the adaptive response of the epithelium and impact on photoreceptors. *Proc. Natl. Acad. Sci. USA* **106**, 18728-18733.
Luo, D. G., Xue, T. and Yau, K. W. (2008). How vision begins: an odyssey. *Proc. Natl. Acad. Sci. USA* **105**, 9855-9862.
Ma, D. K., Marchetto, M. C., Guo, J. U., Ming, G. L., Gage, F. H. and Song, H. (2010). Epigenetic choreographers of neurogenesis in the adult mammalian brain. *Nat. Neurosci.* **13**, 1338-1344.
MacLaren, R. E., Pearson, R. A., MacNeil, A., Douglas, R. H., Salt, T. E., Akimoto, M., Swaroop, A., Sowden, J. C. and Ali, R. R. (2006). Retinal repair by transplantation of photoreceptor precursors. *Nature* **444**, 203-207.
Marquardt, T. and Gruss, P. (2002). Generating neuronal diversity in the retina: one for nearly all. *Trends Neurosci.* **25**, 32-38.
Marquardt, T., Ashery-Padan, R., Andrejewski, N., Scardigli, R., Guillemot, F. and Gruss, P. (2001). Pax6 is required for the multipotent state of retinal progenitor cells. *Cell* **105**, 43-55.
Medina-Martinez, O., Amaya-Manzanares, F., Liu, C., Mendoza, M., Shah, R., Zhang, L., Behringer, R. R., Mahon, K. A. and Jamrich, M. (2009). Cell-autonomous requirement for rx function in the mammalian retina and posterior pituitary. *PLoS ONE* **4**, e4513.
Merbs, S. L., Khan, M. A., Hackler, L., Jr, Oliver, V. F., Wan, J., Qian, J. and Zack, D. J. (2012). Cell-specific DNA methylation patterns of retina-specific genes. *PLoS ONE* **7**, e32602.
Meyer, J. S., Shearer, R. L., Capowski, E. E., Wright, L. S., Wallace, K. A., McMillan, E. L., Zhang, S. C. and Gamm, D. M. (2009). Modeling early retinal development with human embryonic and induced pluripotent stem cells. *Proc. Natl. Acad. Sci. USA* **106**, 16698-16703.
Muranishi, Y., Terada, K. and Furukawa, T. (2012). An essential role for Rax in retina and neuroendocrine system development. *Dev. Growth Differ.* **54**, 341-348.
Nasonkin, I. O., Ward, R. D., Raetzman, L. T., Seasholtz, A. F., Saunders, T. L., Gillespie, P. J. and Camper, S. A. (2004). Pituitary hypoplasia and respiratory distress syndrome in Prop1 knockout mice. *Hum. Mol. Genet.* **13**, 2727-2735.
Nasonkin, I. O., Lazo, K., Hambright, D., Brooks, M., Fariss, R. and Swaroop, A. (2011). Distinct nuclear localization patterns of DNA methyltransferases in developing and mature mammalian retina. *J. Comp. Neurol.* **519**, 1914-1930.
Ng, L., Lu, A., Swaroop, A., Sharlin, D. S., Swaroop, A. and Forrest, D. (2011). Two transcription factors can direct three photoreceptor outcomes from rod precursor cells in mouse retinal development. *J. Neurosci.* **31**, 11118-11125.
Nickells, R. W. and Merbs, S. L. (2012). The potential role of epigenetics in ocular diseases. *Arch. Ophthalmol.* **130**, 508-509.
Nishida, A., Furukawa, A., Koike, C., Tano, Y., Aizawa, S., Matsuo, I. and Furukawa, T. (2003). Otx2 homeobox gene controls retinal photoreceptor cell fate and pineal gland development. *Nat. Neurosci.* **6**, 1255-1263.
Nishiyama, K., Sakaguchi, H., Hu, J. G., Bok, D. and Hollyfield, J. G. (2002). Claudin localization in cilia of the retinal pigment epithelium. *Anat. Rec.* **267**, 196-203.
Ogilvie, J. M., Speck, J. D., Lett, J. M. and Fleming, T. T. (1999). A reliable method for organ culture of neonatal mouse retina with long-term survival. *J. Neurosci. Methods* **87**, 57-65.
Oh, E. C., Cheng, H., Hao, H., Jia, L., Khan, N. W. and Swaroop, A. (2008). Rod differentiation factor NRL activates the expression of nuclear receptor NR2E3 to suppress the development of cone photoreceptors. *Brain Res.* **1236**, 16-29.
Onishi, A., Peng, G. H., Hsu, C., Alexis, U., Chen, S. and Blackshaw, S. (2009). Pias3-dependent SUMOylation directs rod photoreceptor development. *Neuron* **61**, 234-246.
Onishi, A., Peng, G. H., Poth, E. M., Lee, D. A., Chen, J., Alexis, U., de Melo, J., Chen, S. and Blackshaw, S. (2010). The orphan nuclear hormone receptor ERRbeta controls rod photoreceptor survival. *Proc. Natl. Acad. Sci. USA* **107**, 11579-11584.
Osakada, F., Ikeda, H., Mandai, M., Wataya, T., Watanabe, K., Yoshimura, N., Akaike, A., Sasai, Y. and Takahashi, M. (2008). Toward the generation of rod and cone photoreceptors from mouse, monkey and human embryonic stem cells. *Nat. Biotechnol.* **26**, 215-224.
Palczewski, K., Verlinde, C. L. and Haeseleer, F. (1999). Molecular mechanism of visual transduction. *Novartis Found. Symp.* **224**, 191-207.
Poage, G. M., Houseman, E. A., Christensen, B. C., Butler, R. A., Avissar-Whiting, M., McClean, M. D., Waterboer, T., Pawlita, M., Marsit, C. J. and Kelsey, K. T. (2011). Global hypomethylation identifies loci targeted for hypermethylation in head and neck cancer. *Clin. Cancer Res.* **17**, 3579-3589.
Popova, E. Y., Xu, X., DeWan, A. T., Salzberg, A. C., Berg, A., Hoh, J., Zhang, S. S. and Barnstable, C. J. (2012). Stage and gene specific signatures defined by histones H3K4me2 and H3K27me3 accompany mammalian retina maturation in vivo. *PLoS ONE* **7**, e46867.
Raymond, S. M. and Jackson, I. J. (1995). The retinal pigmented epithelium is required for development and maintenance of the mouse neural retina. *Curr. Biol.* **5**, 1286-1295.
Rhee, K. D., Yu, J., Zhao, C. Y., Fan, G. and Yang, X. J. (2012). Dnmt1-dependent DNA methylation is essential for photoreceptor terminal differentiation and retinal neuron survival. *Cell Death Dis.* **3**, e427.
Roberts, M. R., Srinivas, M., Forrest, D., Morreale de Escobar, G. and Reh, T. A. (2006). Making the gradient: thyroid hormone regulates cone opsin expression in the developing mouse retina. *Proc. Natl. Acad. Sci. USA* **103**, 6218-6223.
Robertson, K. D. (2005). DNA methylation and human disease. *Nat. Rev. Genet.* **6**, 597-610.
Roger, J. E., Nellissery, J., Kim, D. S. and Swaroop, A. (2010). Sumoylation of bZIP transcription factor NRL modulates target gene expression during photoreceptor differentiation. *J. Biol. Chem.* **285**, 25637-25644.
Ronaghi, M., Uhlén, M. and Nyrén, P. (1998). A sequencing method based on real-time pyrophosphate. *Science* **281**, 363-365.

Sagdullaev, B. T., Aramant, R. B., Seiler, M. J., Woch, G. and McCall, M. A. (2003). Retinal transplantation-induced recovery of retinotectal visual function in a rodent model of retinitis pigmentosa. *Invest. Ophthalmol. Vis. Sci.* **44**, 1686-1695.

Salero, E., Blenkinsop, T. A., Corneo, B., Harris, A., Rabin, D., Stern, J. H. and Temple, S. (2012). Adult human RPE can be activated into a multipotent stem cell that produces mesenchymal derivatives. *Cell Stem Cell* **10**, 88-95.

Shi, G., Maminishkis, A., Banzon, T., Jalickee, S., Li, R., Hammer, J. and Miller, S. S. (2008). Control of chemokine gradients by the retinal pigment epithelium. *Invest. Ophthalmol. Vis. Sci.* **49**, 4620-4630.

Sonoda, S., Spee, C., Barron, E., Ryan, S. J., Kannan, R. and Hinton, D. R. (2009). A protocol for the culture and differentiation of highly polarized human retinal pigment epithelial cells. *Nat. Protoc.* **4**, 662-673.

Spada, F., Haemmer, A., Kuch, D., Rothbauer, U., Schermelleh, L., Kremmer, E., Carell, T., Längst, G. and Leonhardt, H. (2007). DNMT1 but not its interaction with the replication machinery is required for maintenance of DNA methylation in human cells. *J. Cell Biol.* **176**, 565-571.

Sparrow, J. R., Hicks, D. and Hamel, C. P. (2010). The retinal pigment epithelium in health and disease. *Curr. Mol. Med.* **10**, 802-823.

Strauss, O. (2005). The retinal pigment epithelium in visual function. *Physiol. Rev.* **85**, 845-881.

Swaroop, A., Kim, D. and Forrest, D. (2010). Transcriptional regulation of photoreceptor development and homeostasis in the mammalian retina. *Nat. Rev. Neurosci.* **11**, 563-576.

Swindell, E. C., Bailey, T. J., Loosli, F., Liu, C., Amaya-Manzanares, F., Mahon, K. A., Wittbrodt, J. and Jamrich, M. (2006). Rx-Cre, a tool for inactivation of gene expression in the developing retina. *Genesis* **44**, 361-363.

Wallace, V. A. (2011). Concise review: making a retina – from the building blocks to clinical applications. *Stem Cells* **29**, 412-417.

Winkelmann, J., Lin, L., Schormair, B., Kornum, B. R., Faraco, J., Plazzi, G., Melberg, A., Cornelio, F., Urban, A. E., Pizza, F. et al. (2012). Mutations in DNMT1 cause autosomal dominant cerebellar ataxia, deafness and narcolepsy. *Hum. Mol. Genet.* **21**, 2205-2210.

Wright, A. F., Chakarova, C. F., Abd El-Aziz, M. M. and Bhattacharya, S. S. (2010). Photoreceptor degeneration: genetic and mechanistic dissection of a complex trait. *Nat. Rev. Genet.* **11**, 273-284.

Wu, H. and Zhang, Y. (2011). Mechanisms and functions of Tet protein-mediated 5-methylcytosine oxidation. *Genes Dev.* **25**, 2436-2452.

Yaish, M. W., Colasanti, J. and Rothstein, S. J. (2011). The role of epigenetic processes in controlling flowering time in plants exposed to stress. *J. Exp. Bot.* **62**, 3727-3735.

Young, R. W. (1974). Proceedings: biogenesis and renewal of visual cell outer segment membranes. *Exp. Eye Res.* **18**, 215-223.